Received: 7 March 2024 | Revised: 8 July 2024 | Accepted: 22 July 2024

DOI: 10.1111/wrr.13207

ORIGINAL ARTICLE-REGENERATION SCIENCE

Wound Repair and Regeneration — WILEY

Temporal microbiome changes in axolotl limb regeneration: Stage-specific restructuring of bacterial and fungal communities with a *Flavobacterium* bloom during blastema proliferation

Hanne Altın MS[1] | Büşra Delice MS[1] | Berna Yıldırım PhD[2,3] | Turan Demircan PhD[4] | Süleyman Yıldırım PhD[1,3]

[1]Department of Medical Microbiology, Istanbul Medipol University International School of Medicine, Istanbul, Türkiye

[2]Department of Histology and Embryology, Atlas University School of Medicine, Istanbul, Türkiye

[3]Regenerative and Restorative Medicine Research Center, REMER, İstanbul Medipol University, İstanbul & Research Institute for Health Sciences and Technologies (SABITA), Istanbul Medipol University, Istanbul, Türkiye

[4]Medical Biology Department, Muğla Sıtkı Koçman University School of Medicine, Muğla, Turkey

Correspondence
Süleyman Yıldırım, Department of Medical Microbiology, Istanbul Medipol University International School of Medicine, Istanbul, Türkiye.
Email: suleymanyildirim@medipol.edu.tr

Funding information
Medipol University Research Fund

Abstract

The intricate relationship between regeneration and microbiota has recently gained attention, spanning diverse model organisms. Axolotl (*Ambystoma mexicanum*) is a critically endangered salamander species and a model organism for regenerative and developmental biology. Despite its significance, a noticeable gap exists in understanding the interplay between axolotl regeneration and its microbiome. Here, we analyse in depth bacterial 16S rRNA amplicon dataset that we reported before as data resource and profile fungal community by sequencing ITS amplicons at the critical stages of limb regeneration (0–1–4–7–30–60 days post amputation, 'dpa'). Results reveal a decline in richness and evenness in the course of limb regeneration, with bacterial community richness recovering beyond 30 dpa unlike fungi community. Beta diversity analysis reveals precise restructuring of the bacterial community along the three phases of limb regeneration, contrasting with less congruent changes in the fungal community. Temporal dynamics of the bacterial community highlight prevalent anaerobic bacteria in initiation phase and *Flavobacterium* bloom in the early phase correlating with limb blastema proliferation. Predicted functional analysis mirrors these shifts, emphasising a transition from amino acid metabolism to lipid metabolism control. Fungal communities shift from *Blastomycota* to *Ascomycota* dominance in the late regeneration stage. Our findings provide ecologically relevant insights into stage specific role of microbiome contributions to axolotl limb regeneration.

KEYWORDS
axolotl, *Flavobacterium*, limb, microbiome, regeneration

1 | INTRODUCTION

The axolotl (*Ambystoma mexicanum*), a species facing critical endangerment in its natural habitat, is a member of the *Ambystoma* clade

Hanne Altın and Büşra Delice are equal contribution.

within the mole salamander family (*Ambystomatidae*). Distinguishing salamanders from other amphibians is their remarkable capacity for complete regeneration, encompassing not only limbs and appendages but also certain internal organs. The intricate cellular and molecular mechanisms involved in the extensively researched limb regeneration of axolotls make it a topic of significant scientific interest.[1,2]

To regenerate its limbs, the axolotl employs a fascinating process involving the generation of blastema cell mass, resembling the embryonic limb bud. This intricate procedure is significantly influenced by innervation, where the blastema acts as the driving force for redevelopment through a combination of growth and redifferentiation. Despite its complexity, limb regeneration in axolotls unfolds systematically in a stepwise manner. Indeed, it is well established that the regeneration progresses over distinct interdependent stages according to morphogenesis.[3] These sequential phases encompass wound healing, dedifferentiation (highlighted by blastema establishment) and re-development stages of regeneration, respectively.[4–6] The cell lineage- and regeneration stage-specific expression patterns of various morphogenesis genes are critical for successful limb regeneration and the early steps are highly critical for determining the extent of regenerative response after limb amputation. More specifically, after limb amputation, a specialised wound epidermis forms within ~24 h through cell migration. Wound epidermis is structurally and molecularly distinct from fully differentiated, intact epidermis. Innervated wound epidermal cells then thicken the tissue, dermal cells migrate beneath it, and proliferates. In the days following re-epithelialisation, progenitor cells enter into the cell cycle as well as the accumulate at the tip of the stump, beneath the wound epidermis. These progenitor cells may originate from stem cells or by dedifferentiation. Epigenetic regulation controls both wound epidermis formation without scarring and epithelial-to-mesenchymal transition.[1,7,8] Together, the activated cells accumulated at the tip of the stump give rise to highly proliferative blastema cells.[1,7,9]

Timing of these events may slightly vary in different salamander species but in axolotl the movement of cells from the dermis into the early limb blastema begin to migrate beneath the wound epithelia for about 5 days post amputation (dpa0-5: 'initiation phase'). Next, the wound epithelium thickens and forms an apical epithelial cap (AEC), which promotes the generation of a population of undifferentiated mesenchymal cells called a 'blastema', which is formed through a 'dedifferentiation' process from differentiated tissues (dpa6-20: 'early phase'). In the re-development stage, the blastema continues to grow distally via cellular proliferation until the completion of regeneration (dpa21-30: 'late phase').[4–6,10,11]

Animal microbiomes play key roles in an animal's development, health, behaviour, and protection from pathogens.[12–15] Recently, the impact of the host microbiome on regenerative ability of its tissues, organs or even whole-body has gained significant attention even though this is still relatively a new area of research in the field of microbiomes. Indeed, several species, renowned for their regenerative capabilities, such as planarians, sea cucumber, and zebrafish, have been employed in research to investigate whether the microbiome plays a role in regulating the regenerative potential of these hosts or is directly engaged in the regeneration process. These studies revealed that some bacterial species were shown to be causally linked with the regenerative ability of the model animals. For instance, *Pseudomonas* and *Aquitalea* species on Planaria, *Erwinia carotovara* on fruit fly, *Aeromonas veronii* on Zebrafish, *Akkermansia muciniphila* and some probiotic *Lactobacillus species* in intestinal cell proliferation.[16] The microbiome, therefore, influence tissue regeneration by modulating immune responses and inflammation, and potentially contributing to the activation of regenerative pathways.

The axolotl is a permanently aquatic animal and its amputated limb regenerates against the backdrop of microbial communities of the aquaria. This raises the question as to whether and how axolotl's gut and skin microbiota and water microbiota in the aquarium tank impact limb regeneration. Remarkably, however, reports on the impact of the microbiome on this highly regenerative animal, the axolotl, and salamanders at large, are very limited, leaving a significant knowledge gap. We previously generated a high-quality 16S rRNA dataset from longitudinal sampling of axolotl limb tissues over the course of regeneration stages and exceptionally presented the dataset to the interest of the axolotl scientific community.[17]

In this study, we comprehensively analyse the diversity and temporal dynamics of both bacterial and fungal communities within the same experimental setup. We hypothesised that regenerating limb microbial communities are distinct from the environment; host factors create unfavourable environment for the colonisation of pathogens and induce the microbial communities to progressively adapt to evolving micro-niches in the course of axolotl limb regeneration. Our results demonstrate that both bacteria and fungi communities dramatically restructure over the course of axolotl limb regeneration stages and show lack of resilience at the fully regenerated stage. Our findings also provide evidence that the host limb tissues select microbial taxa that can colonise in the regenerated tissues.

2 | MATERIALS AND METHODS

2.1 | Ethical statement and experimental design

The ethical statement and experimental design were previously described in our previous report.[17] Briefly, this study was conducted at the Regenerative and Restorative Medicine Research Center (REMER) of the Istanbul Medipol University. Experimental protocols and animal care conditions were approved by the local ethics committee of Istanbul Medipol University (the authorisation number 38828770–604.01.01-E.10834). The founders of the initial axolotls colony were procured from the University of Kentucky, USA, and reared in optimised conditions[18] in aquaria in the animal care facility of the university.

A total of 54 axolotls were selected at random from a group of siblings. The randomly selected animals were then individually housed in aquariums filled with Holtfreter's solution at a constant temperature of 18 ± 2°C. They were fed with standard food (JBL Novo LotIM) once daily. The experimental design, shown in Figure 1, included nine

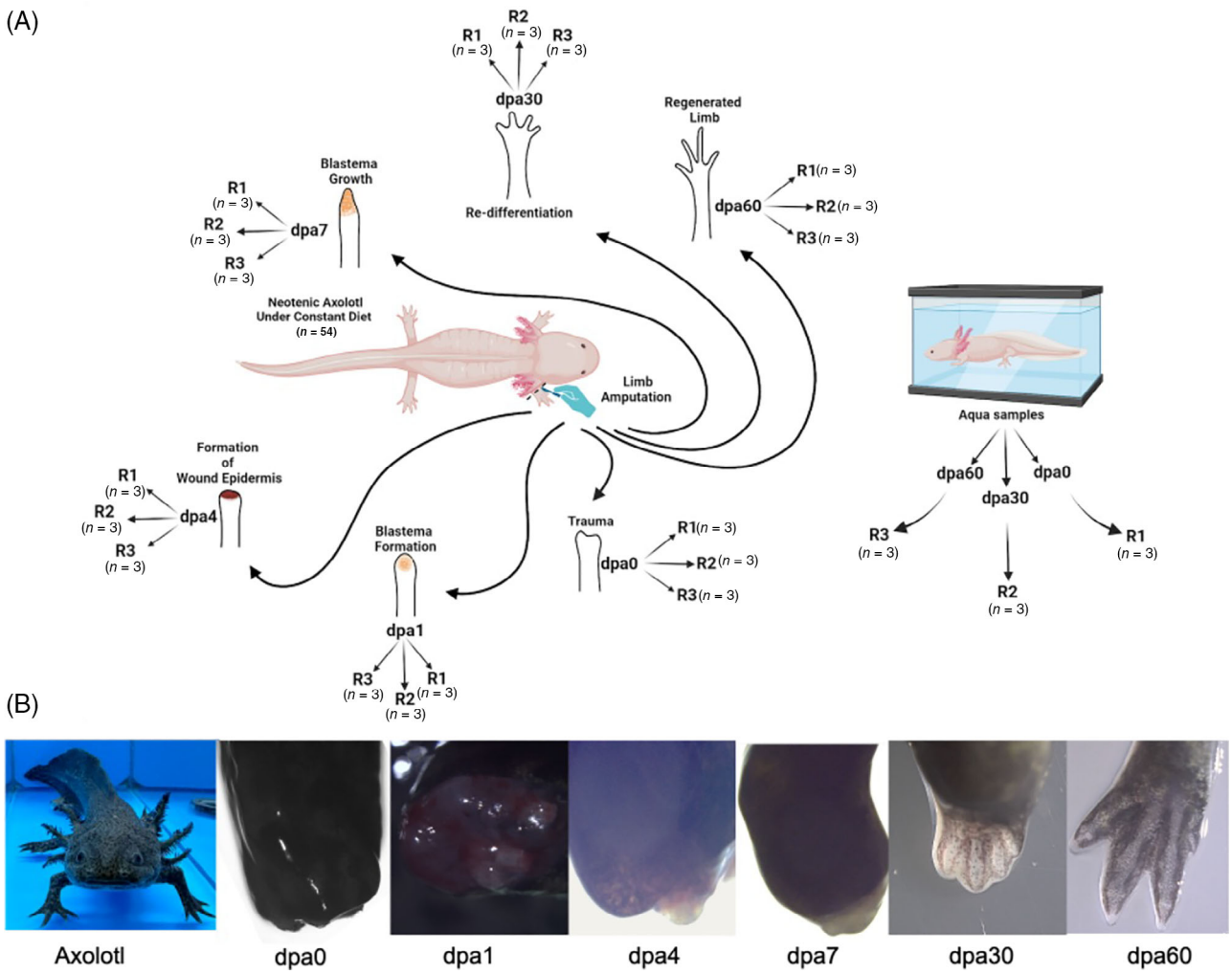

FIGURE 1 (A) Experimental layout. The study involved sequencing 16S rRNA and ITS1 amplicons from 21 samples, comprising 18 limb tissue samples and 3 samples of aquarium water. Limb tissue samples were obtained post-amputation at various time intervals: dpa0, dpa1, dpa4, dpa7, dpa30, and dpa60 (where 'dpa' denotes days post-amputation). Each time point included 3 biological replicates (R1, R2, and R3), wherein each replicate constituted pooled limb tissue samples from 3 animals to mitigate interindividual variability. Aquarium water samples were collected at 3 time intervals (day 0, day 30, and day 60) with 3 replicates (R1, R2, and R3) each. Adapted with permission from Demircan et al. 2019. (B) Images of Axolotl and amputated limbs, sourced from unrelated experiments involving different animals.

animals per group, divided into three biological replicates (R1, R2, R3) to assess reproducibility. During the study, each animal was kept in a separate aquarium. Limb amputation involved anaesthetising the axolotls with 0.1% Tricaine methane sulfonate (Cat. No. E10521 or MS-222, Sigma-Aldrich, St. Louis, MO, USA) and amputating the right forelimb at the mid-zeugopod level.

2.2 | Sample collection

After amputation, animals were randomly assigned to six groups, simulating axolotl limb regeneration phases: initiation (dpa 0 and dpa 1), early (dpa 4 and dpa 7), and late (dpa 30 and dpa 60). Tissue samples from three animals were pooled to reduce variation, cryopreserved in liquid nitrogen, and stored at −80°C until genomic DNA isolation. Sampling specifics included 1 mm tissue around the cut site for dpa 0 and dpa 1, removal of newly formed blastema and 0.5 mm posterior tissue for dpa 4 and dpa 7, and collection around the original cut site for dpa 30 and dpa 60 to analyse microbiota in regenerated tissues.

To explore microbiota colonisation in axolotl limbs originating from Holtfreter's solution, we collected water samples (100 mL) from a total of 9 individual aquaria in the course of the experimental timeline. We pooled water samples from aquaria of 3 axolotls at the beginning (day0-R1), 3 water samples in the middle (day30-R2), and 3 at the end (day60-R3) and named these samples the 'aqua' control group, resulting 3 replicates (R1, R2, R3; Figure 1A).

2.3 | DNA extraction and amplicon sequencing

Genomic DNA was isolated from skin tissue samples using the DNeasy Blood and Tissue Kit (Qiagen, Catalogue No. 69504), while

the Metagenomic DNA Isolation Kit (Epicentre, catalogue no: MGD08420) was employed for Aquarium water samples. The concentration of the isolated genomic DNA was measured using the Qubit 2.0 Fluorometer (Thermo Fisher Scientific, MA, USA). The internal transcribed spacer 1 (ITS1) region primers (ITS1-30F: GTCCCTGCCCTTTGTACACA and ITS1-217R: TTTCGCTGCGTTCTTCATCG) were selected from a previously published report[19] and V3-V4 region of 16S rRNA gene was amplified in the previous study as described before.[17] To ensure DNA integrity, an aliquot of the samples was run on a 1.0% agarose gel. For each sample, PCR was performed in a total volume of 25 μL with two replicates, including approximately 12.5 ng of purified DNA template and 2x KAPA HiFi HotStart Ready Mix. The PCR conditions consisted of an initial denaturation at 95°C for 3 min, followed by 25 cycles of denaturation at 95°C for 30 s, annealing at 55°C for 30 s, and extension at 72°C for 30 s. The final extension was at 72°C for 5 min. Negative controls in genomic DNA isolation and PCR steps were included to control potential contamination and sequenced along with the other samples.

Amplicons were purified using the Agencourt AMPure XP purification system (Beckman-Coulter Cat. No. A63881, USA). A second PCR, with eight cycles, was conducted using sample-specific barcodes, and the obtained amplicons were purified again. Equimolar concentrations from each library were pooled and sequenced on an Illumina MiSeq sequencer using the MiSeq Reagent Kit v2 (500 cycles). Raw data from this sequencing effort can be found in the NCBI Sequence Read Archive (Accession number: PRJNA1073213).

2.4 | Sequence processing pipeline and taxonomic classification

Pair-end reads of the amplicons were first merged using cutadapt[20] after removing primers and low-quality sequences. The merged clean sequence reads were then uploaded to the Nephele platform (v.2.30, http://nephele.niaid.nih.gov) to run the DADA-ITS pipeline and 16S rRNA pipeline on default parameters and their associated denoising and removing chimeric reads. For taxonomic assignment of the reads the SILVA small-subunit rRNA sequence database (v.132)[21] for bacteria and the database for Fungi[22] were used. To run the Phylogenetic investigation of communities by reconstruction of unobserved states (PICRUSt2)[23] analysis we locally reran QIIME2 on Greengenes taxonomy. The resulting amplicon sequence variants (ASVs) table was filtered to exclude chloroplasts, mitochondria, archaea, eukaryotes, or unknown reads were eliminated. As the number of sequences per sample was quite imbalanced, we rarefied ASV tables before starting the downstream analyses and applied center log ratio (CLR) transformation. Downstream analysis of ASVs was carried out using the package Phyloseq[24] in R version 4.1.0.

2.5 | Community structures and diversity

The alpha diversity at each sampling time point was calculated using Chao1, Shannon, and Simpson metrics. The Kruskal-Wallis (KW) test and posthoc Dunn's test were used to identify alpha diversity differences between samples. To test whether bacterial and fungal communities differ in community composition and structure we employed Canonical analysis of principal coordinates (CAP) based on Bray-Curtis distance matrix. Statistically significant differences among life stages were determined with permutational ANOVA (PERMANOVA) performed with adonis function. To test pairwise group differences were tested using pairwise.adonis wrapper function for multiple testing 999 in vegan R package and p values were corrected with False Discovery Rate (FDR) for multiple testing. Indicator species analysis was performed using the indicspecies package in R. Spearman rank-based correlation coefficients were calculated using from the Hmisc R package. Moreover, pheatmap, lattice, UpSetR and ggplot2 R packages were used for visualisations. Longitudinal changes of taxa of interest was plotted using LOESS() function that fits local polynomial regression within stats (v3.6.2) and ggplot2 R packages. We established microbial co-abundance relationships by combining the SparCC[25,26] algorithm with 20 iterations to infer linear relationships.

3 | RESULTS

In our previous work, we provided a comprehensive overview of the experimental design employed in this study, as well as the 16S rRNA dataset generated and shared with the scientific community for further analysis or meta-analysis.[17] Expanding on this groundwork, we broadened our inquiry by analysing ITS1 amplicons from identical archival gDNA samples to characterise the temporal changes of the mycobiome during the various stages of limb regeneration. These stages were categorised as dpa0–dpa1 for the initiation phase, dpa4–dpa7 for the early phase, and dpa30–dpa60 for the late phase. In this study, we provide a comprehensive analysis of both bacterial and fungal communities simultaneously.

Briefly, we meticulously monitored the amputated axolotls for 60 days and longitudinally collected a total of $n = 21$ samples (comprising 18 limb tissue samples from $n = 54$ adult axolotls and 9 individual aquaria samples with replicates) in total (Figure 1). Subsequent to preprocessing ITS amplicon sequences, conducting quality checks, and removing chimeric sequences using the DADA2 pipeline we obtained 238 amplicon sequence variants (ASVs) with sufficient sequencing depth (28,978 reads/sample in the rarefied (ASVs) table). The bacteria ASV table included 116,220 reads/samples in the rarefied ASV table.

3.1 | Dynamic restructuring of bacterial and fungal diversity across regeneration stages

We compared species richness and diversity using a variety of alpha-diversity indices including Chao1, Shannon, and Simpson and observed consistent decreasing trend in all metrics of both bacterial diversity (Figure 2A) and fungal diversity (Figure 2B). Unlike fungal community bacterial richness did not reach significance level among samples despite the apparently decreasing trend as measured by

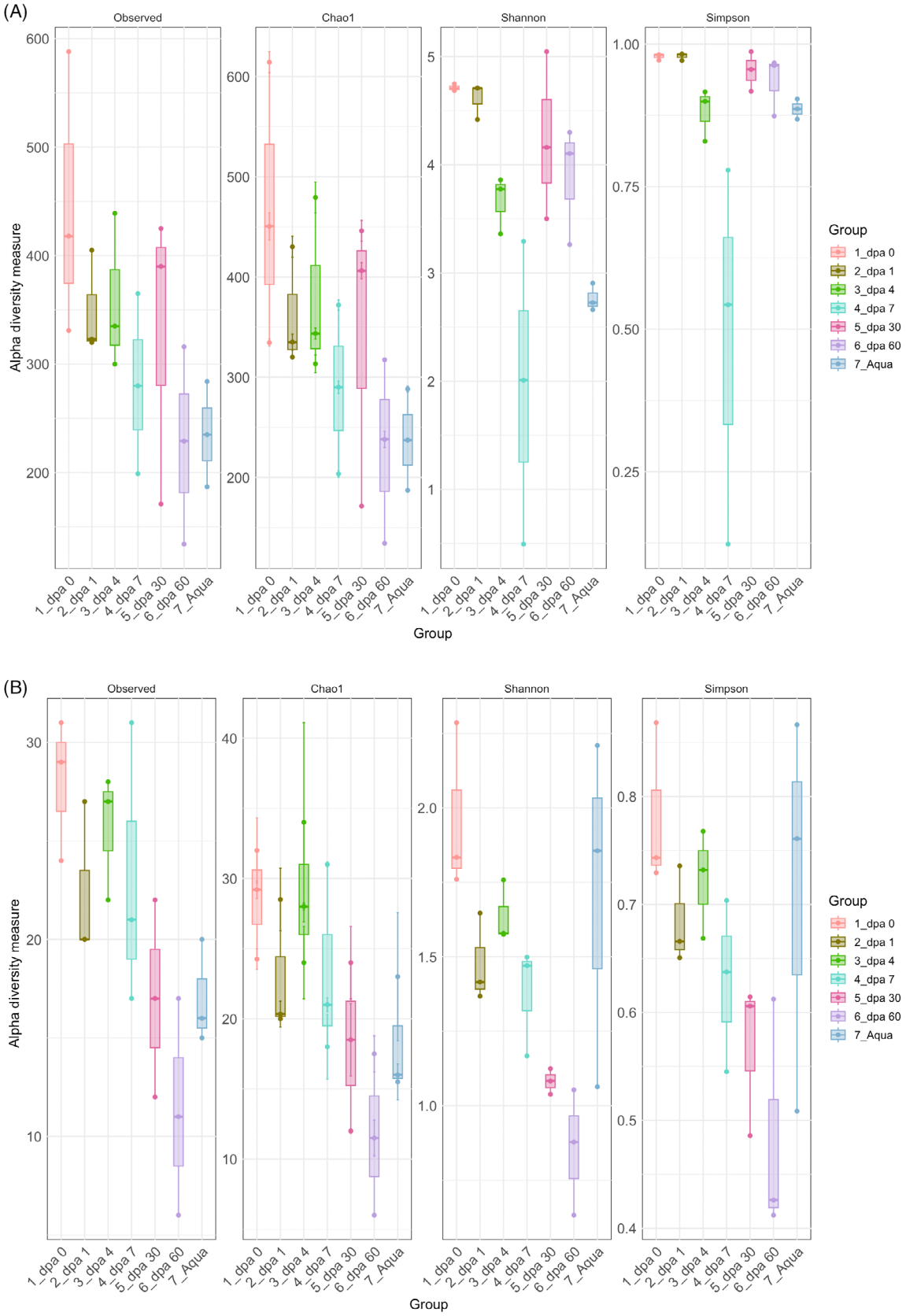

FIGURE 2 (A, B) Longitudinal representation of alpha diversity metrics of bacterial and fungal communities. (A) Box plots displaying alpha diversity metrics for bacterial communities, including observed Operational Taxonomic Units (OTUs), Chao1, Shannon, and Simpson indices. (B) Box plots illustrating alpha diversity metrics for fungal communities, encompassing observed Operational Taxonomic Units (OTUs), Chao1, Shannon, and Simpson indices. The boxes denote interquartile ranges (IQR) with the median as a black line. Statistical analyses were conducted using the Kruskal-Wallis test followed by post hoc Dunn's test for comparison (For more details, refer to Supplementary file, Table S1).

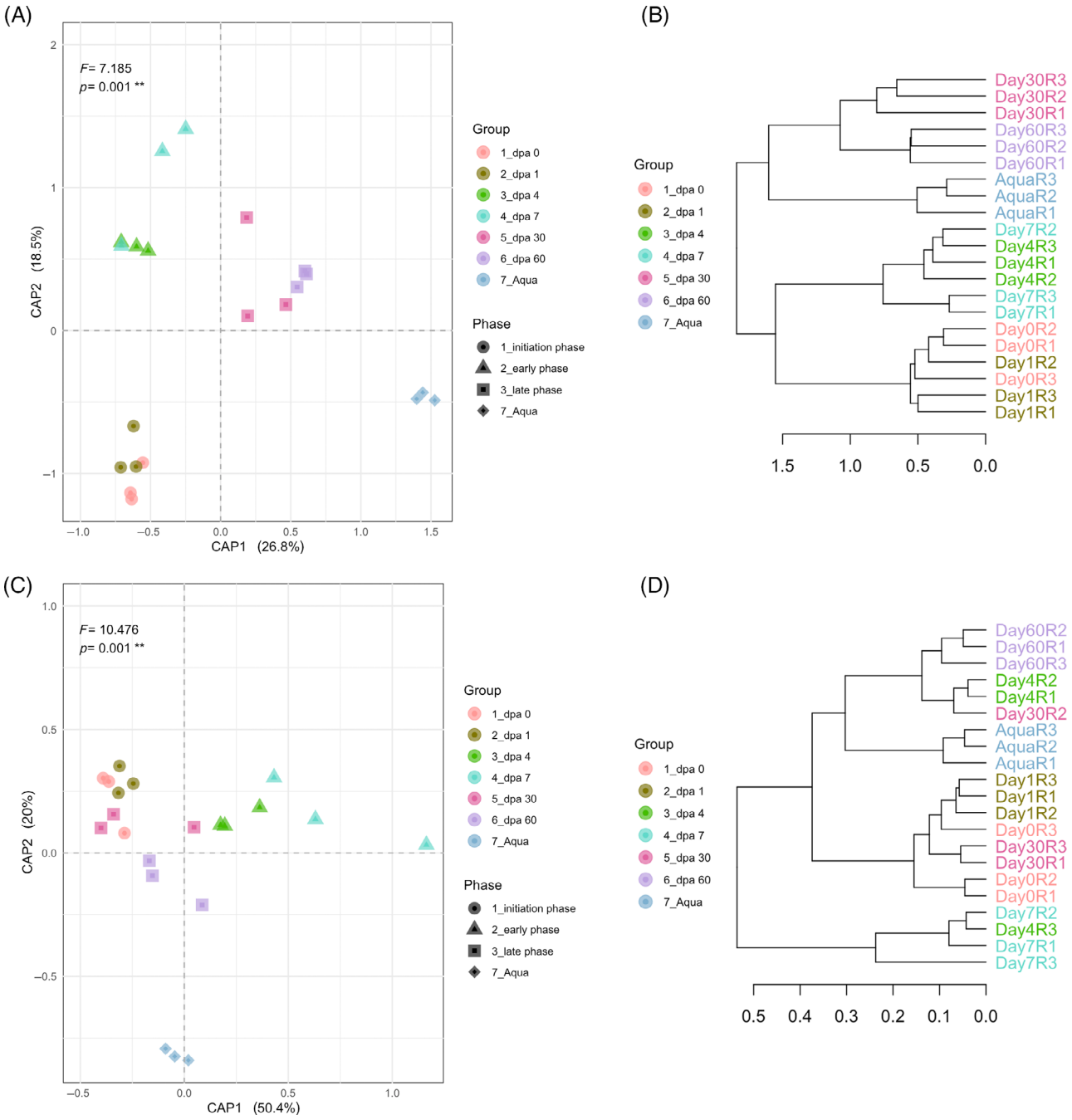

FIGURE 3 (A, B) Beta diversity and clustering analysis of bacterial communities associated with regenerating axolotl limb tissues. (A) Constrained Analysis of Principal Coordinates (CAP) was conducted to examine the beta diversity of ASV abundances across all study samples. The chart was created utilising the Bray-Curtis distance metric and CAP ordination method. Each group is visually differentiated by colour, with distinct shapes representing the phases of axolotl limb regeneration. Permutational multivariate analysis of variance (PERMANOVA) was used to test the multivariate null hypotheses of no differences among a priori defined groups ($F = 7.191$, $p = 0.001$). Permutational analysis of multivariate dispersions (PERMDISP) was used to test for heterogeneity of community structure in a priori groups ($p = 0.099$). (B) Hierarchical clustering of samples based on beta-diversity analysis of ASV abundances was performed using Ward's method. Coloured clades in the dendrogram indicate significant bifurcations, based on the SIMPROF significance test (significance level 5%, 999 permutations). (C, D) Constrained analysis of principal coordinates (CAP) model of predicted bacteria functional abundances using PICRUSt2 and Clustering analysis. (C) Constrained Analysis of Principal Coordinates (CAP) was conducted to examine the beta diversity of ASV abundances across all study samples. The chart was created utilising the Bray-Curtis distance metric and CAP ordination method. Each group is visually differentiated by colour, with distinct shapes representing the phases of axolotl limb regeneration. Permutational multivariate analysis of variance (PERMANOVA) was used to test the multivariate null hypotheses of no differences among a priori defined groups ($F = 10.461$, $p = 0.001$). Permutational analysis of multivariate dispersions (PERMDISP) was used to test for heterogeneity of community structure in a priori groups ($p = 0.048$). (D) Hierarchical clustering of samples based on Beta-diversity analysis of ASV abundances was performed using Ward's method. Coloured clades in the dendrogram indicate significant bifurcations, based on the SIMPROF significance test (significance level 5%, 999 permutations).

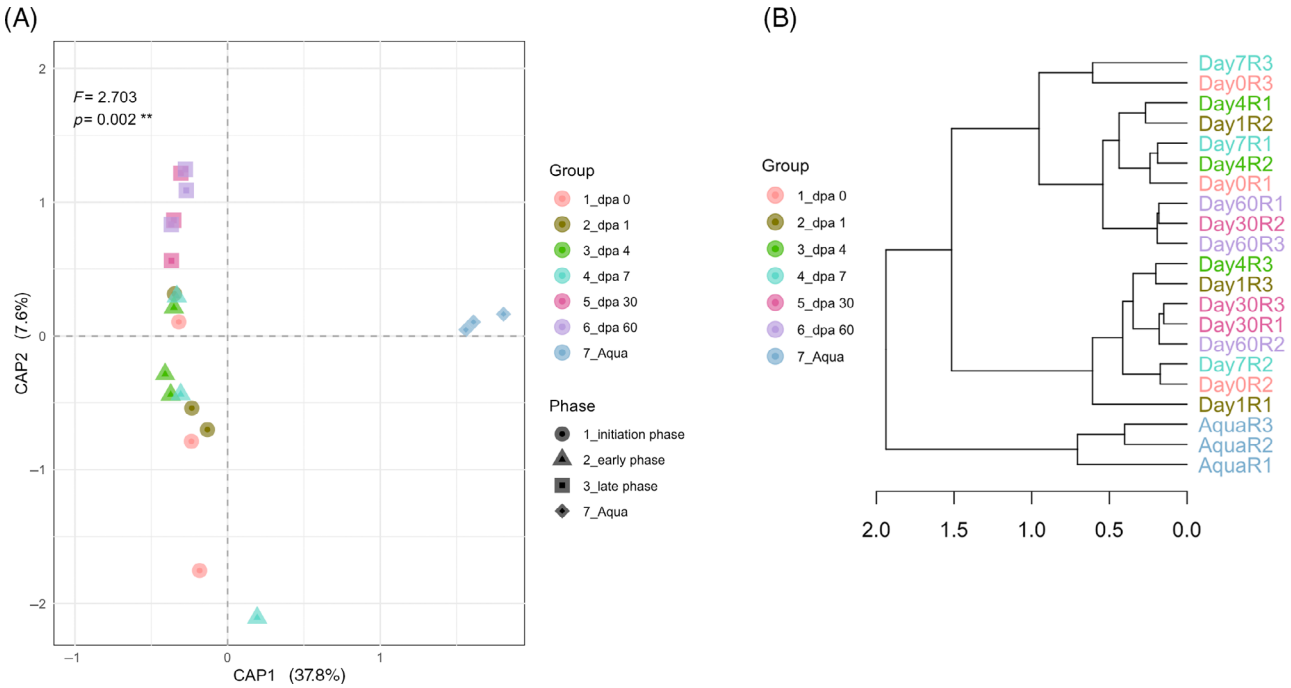

FIGURE 4 (A, B) Beta diversity and clustering analysis of fungal communities associated with regenerating axolotl limb tissues. (A) Canonical analysis of principal coordinates (CAP) plot illustrating dissimilarities of fungal communities in the axolotl limb tissue samples. The plot was created utilising the Bray-Curtis distance metric and CAP ordination method. Each group is visually differentiated by colour, with distinct shapes representing the phases of axolotl limb regeneration. (PERMANOVA, $F = 2.715$, $p = 0.004$; PERMDISP $p = 0.5855$). (B) Hierarchical clustering of samples based on Beta-diversity analysis of ASV abundances was performed using Ward's method. Coloured clades in the dendrogram indicate significant bifurcations, based on the SIMPROF significance test (significance level 5%, 999 permutations).

Observed species and Chao1 indices (KW, $p > 0.05$, Table S1.1). In contrast, Shannon and Simpson indices steeply increased at dpa30 and dpa60 (late phase or re-development of the limbs, KW, $p = 0.01375$ for Shannon and $p = 0.01423$ for Simpson), suggesting bacteria community colonising the re-growing limb skin was more evenly restructured than fungal community despite the decrease in the number of species. Indeed, Dunn's posthoc pairwise comparisons for each alpha diversity index for bacterial community showed significant differences between all sample types except between the samples of the initiation phase and late phase while this pattern was absent for the fungal community samples (Tables S2.1–S2.2).

Next, we analysed temporal dynamics of both bacteria and fungi communities using Bray Curtis distance and Canonical Analysis of Principal Coordinates (CAP) (Figure 3A), a constrained ordination that maximises the differences among a priori groups. We reproduced our prior findings,[17] indicating distinct separation among bacterial communities at each sampling time point (PERMANOVA, $p = 0.001$, pseudo-$F = 7.191$), a result further bolstered by statistically significant hierarchical clustering (Figure 3B) and confirmed by the SIMPROF significance test (significance level 5%, 999 permutations). These results were mirrored by the CAP and cluster analysis predicted metagenome functional pathway abundances (PICRUSt2) (Figure 3C,D), PERMANOVA, pseudo-$F = 10.461$, $p = 0.001$ and SIMPROF (5%, 999 permutations, respectively). Interestingly, despite the significant differences in distances between centroids of fungal community samples (Pseudo-$F = 2.715$, $p = 0.004$, Figure 4A), both hierarchical clustering (Figure 4B) and pairwise PERMANOVA analysis (using Monte Carlo permutation) revealed that fungal communities did not exhibit significant separation at any pairs of dpa timing points ($p > 0.05$), unlike the pairwise contrasts observed in bacterial communities ($p < 0.05$) (Table S3). This analysis suggests that the spatial and temporal dynamics of the fungal community in response to regeneration are distinct from those of the bacterial community.

3.2 | Regeneration stages prompt restructuring of bacterial communities, triggering *Flavobacterium* bloom

The heatmap of Top20 most abundant bacteria taxa at genus level showed conspicuous clustering of co-abundant taxa by the limb regeneration stages of axolotl (Figure 5). In the initiation stage (dpa0-1) largely anaerobic gut bacteria (*Bacteroides*, *Akkermansia*, *Paenarthrobacter*, *Odoribacter*, *Parabacteroides*, and unclassified species within the family of *Ruminococcoaceae* and *Lachnospiraceae*) were clustered together while in the early phase (dpa4-7) a bloom of *Flavobacterium* was observed. Finally, in the late phase (dpa30-60) the bacterial profile continued to evolve, giving rise to the potentially opportunistic bacteria (e.g. *Staphylococcus*, *Pseudomonas*) or taxonomically closely related species that are often isolated from soil

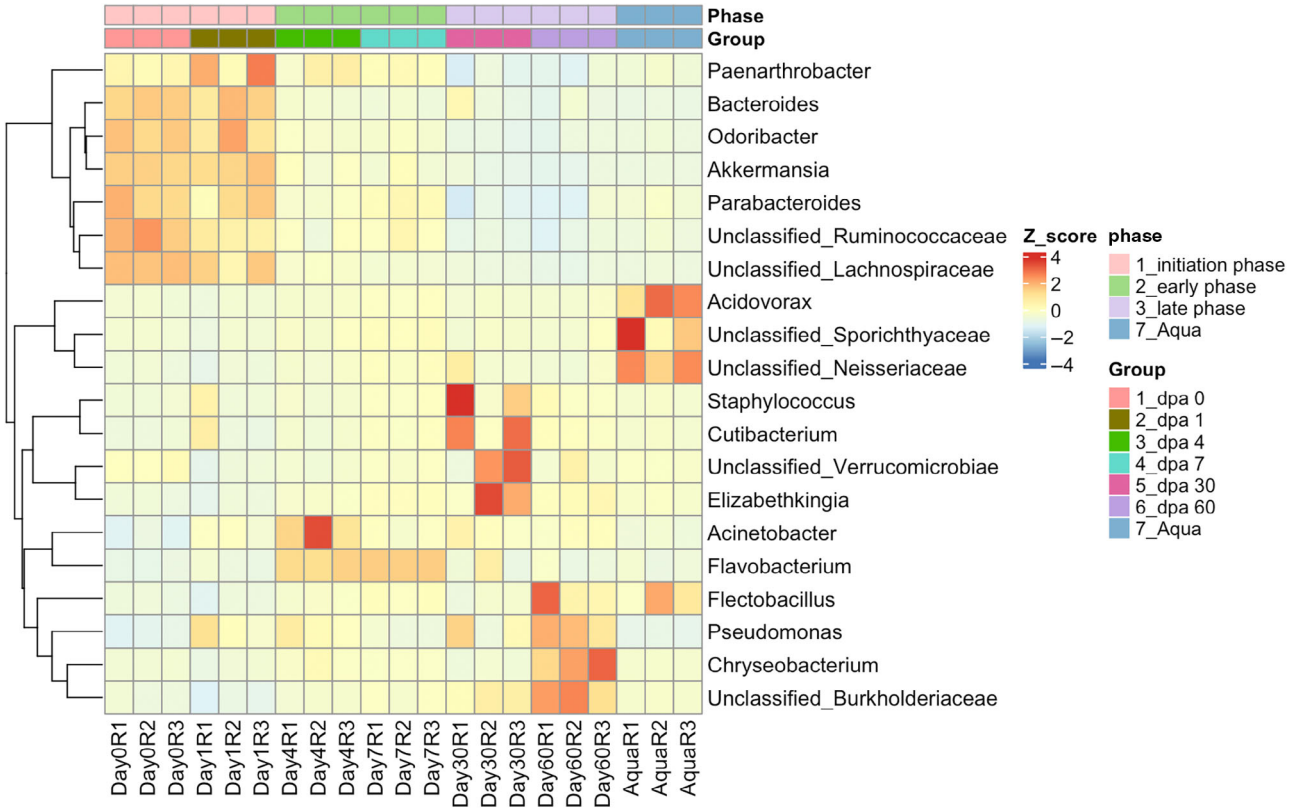

FIGURE 5 Heatmap depicting the relative abundance of the top 20 abundant bacterial taxa during axolotl limb regeneration over time. Hierarchical clustering using complete linkage with Ward's method is illustrated by the dendrogram, highlighting patterns of similarity in taxonomic composition across different time points.

freshwater creeks, lakes (e.g. *Elizabethkingia* and *Chryseobacterium* in the order of *Flavobacteriales*) that colonise on the skin of the re-growing limbs.

Furthermore, we employed LOESS regression, which uses weighted local polynomials to model species abundance data across time, to demonstrate longitudinal shifts of Top20 taxa. Clearly, in the early phase (dpa4-7) a bloom of *Flavobacterium* persisted during the critical early stage that allows for the formation and growth of blastema (Figure 6). A significant increase in the abundance of *Chryseobacterium* over dpa60 was also remarkable. Additionally, we performed indicator species analysis to unravel indicator taxa at each sampling time point (Figure 6B), which further supported that *Flavobacterium* is indeed an indicator taxon of the early phase, a critical window for blastema to start proliferating. Notably, *Aquabacterium* and *Acinetobacter* were also found to be an indicator taxa within the early phase although their abundances were low. To answer the question of whether functional pathway abundances of bacteria communities follow a similar trend as taxa in the course of limb regeneration stages we plotted the prediction of metagenome functional pathway abundances (PICRUSt2) in a heatmap (Figure 7). Remarkably, we observed the clustering of pathways by limb regeneration stages, mirroring the taxa abundance trend. The pathways in the initiation phase were found to be largely associated with amino acid and nucleic acid biosynthesis while lipid biosynthetic pathways dominated the following early phase. The late phase did not show clustered pathways. Correlation analysis between abundances of bacteria taxa and pathways highlighted *Chryseobacterium* and *Flavobacterium* highly significantly associated with the amino acid and lipid pathways, respectively ($r = 0.40$, $p < 0.05$, Figure S1). Together, the diversity and co-abundance of bacteria communities and their clustered pathways point toward stage specific restructuring of bacterial communities across the limb regeneration while restructuring of the fungal communities does not closely follow the regeneration stages.

3.3 | Unexpected complexity of fungal communities during the course of limb regeneration and co-abundance network analysis

The lack of obvious restructuring trend within fungal community was also manifested in the taxonomic diversity of fungal communities. In spite of significant shift in community composition from Basidiomycota dominance to Ascomycota prevalence (Figure 8A) genus level fungal taxa did not cluster by the stages of limb regeneration (Heatmap, Figure 8B). These findings prompted us to investigate degree of temporal relationship between bacterial and fungal communities. We therefore performed Procrustes analysis and Mantel correlation between the Bray-Curtis distance matrices for both

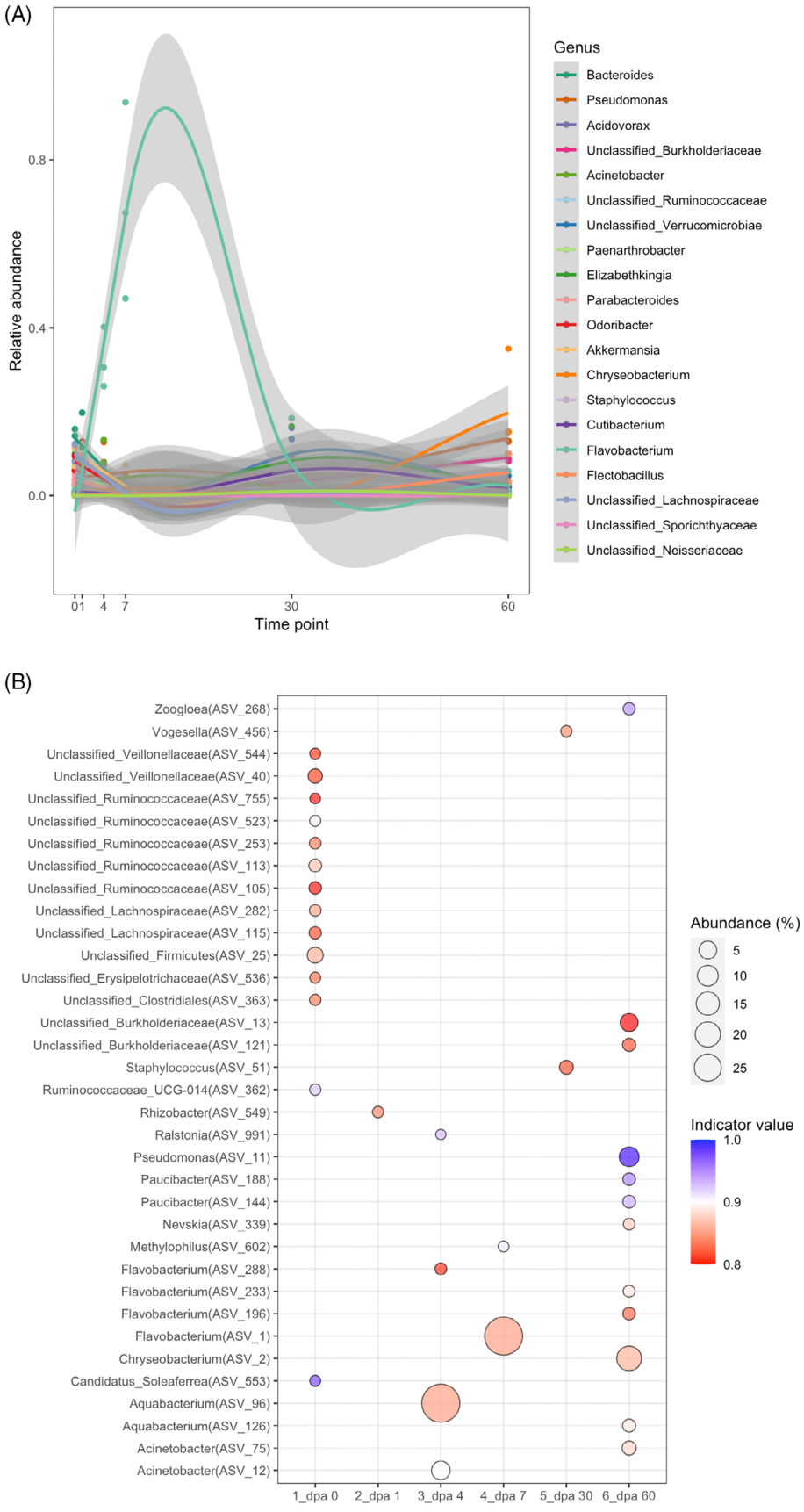

FIGURE 6 Legend on next page.

communities. Interestingly, both Procrustes and Mantel analyses identified a moderately significant relationship between the two datasets (Procrustes correlation = 0.73, $p = 0.001$ and Mantel test $r = 0.69$, $p = 0.001$), suggesting both communities influence each other during regeneration. In addition, we found significant correlations (r = ±0.40, $p < 0.05$) between bacteria and fungi taxa (Figure 7). In addition to *Flavobacterium*, *Unclassified Neisseriaceae*, *Chryseobacterium*, *Elizabethkingia*, *Unclassified Burkholderiaceae*, and *Akkermansia* exhibited significant correlations with fungal taxa. Notably, *Flavobacterium* and *Unclassified Burkholderiaceae* showed predominantly negative correlations. Among fungal taxa, *Talaromyces*, *Aspergillus*, and *Stachybotrys* displayed significant correlations with bacterial taxa (Figure S2A). These correlations prompted us to analyse how the co-abundance network of bacteria and fungi community restructure during the initiation, early, and late phases of axolotl limb regeneration (Figure S2B). We employed SparCC correlation, which uses the centered log-ratio transformation to address data compositionality[25] to infer co-abundance relationship of top20 most abundant bacteria and fungi. In the initiation, early, and late phases, the modularity and average clustering coefficients were 0.827, 0.644, 0.788, and 0.571, 0.418, 0.492, respectively. These values suggest that interkingdom interactions within and between all three phases are robust, with specific interacting taxa within each module forming tight-knit groups. Notably, these groups restructure in each phase, establishing new connections throughout the host regeneration process. For example, during the initiation phase, one of the largest interacting groups, including *Flectobacillus*, unclassified *Lachnospiraceae*, *Malasseziaceae_gen_Incertae_sedis*, and *Absconditonia*, disappears in the early phase as its members form new connections with other taxa. Indeed, *Flectobacillus* and *Flavobacterium* positively interact with each other while potentially inhibiting *Spizellomycetales_gen_Incertae_sedis*, a fungus in the phylum Chytridiomycota, which also includes *Batrachochytrium dendrobatidis* (Bd), the causative agent of chytridiomycosis in amphibians. In the late phase, *Flectobacillus* shows a negative correlation with *Aspergillus*, whereas the correlation with *Flavobacterium* becomes insignificant. The functional role of these interactions, however, warrants further research in the context of axolotl limb regeneration.

Finally, since Aqua samples were placed farther away from the limb tissue samples in CAP figures we compared the number of unique and shared taxa between limb tissue and aqua samples (Figure 8A,B). The upset figures shows both bacterial and fungal communities are substantially unique at each sampling points (dpa0-dpa60) and few taxa persisted as shared species between these time points, pointing toward highly dynamic temporal shifts of the community compositions over the course of the limb regeneration. As shown in Figure 8A the highest number of unique bacterial species assembled at dpa0 (562 ASVs) and dpa30 (535 ASVs) and 36 ASVs are common among the sampling points. As expected, only 14 ASVs are present both in Aqua water and all limb tissues, suggesting the temporal dynamics of the microbiota colonising regenerating tissues is due largely to the host selection although microbe-microbe interactions could also contribute to unique community profiles.

4 | DISCUSSION

The axolotl, with its remarkable ability to regenerate limbs and organs due to sustained neoteny, has strongly attracted the attention of scientific community for translational medicine research.[3] Despite its recently sequenced expansive genome,[27] studies on the axolotl microbiome are very limited. In this pioneering study, we unveil, for the first time, the substantial restructuring of both fungal and bacterial communities throughout the intricate process of limb regeneration. Our findings illuminate the emergence of temporally unique community compositions at sampling days that correspond to the widely accepted three phases of limb regeneration in axolotls. Remarkably, as the axolotl's limbs undergo full regeneration, the microbial communities inhabiting the limb skin undergo significant turnover. This suggests that the axolotl limb skin microbiome lacks resilience in response to the regenerative process. Such insights into the dynamic interplay between microbial communities and the regenerative capacity of axolotls shed new light on the intricate mechanisms underlying limb regeneration. Moreover, they offer valuable implications for translational research aimed at harnessing the regenerative potential of axolotls for therapeutic purposes in humans.

One of the most striking observations on limb microbiota is regeneration-induced changes in richness and evenness of limb microbiota as evidenced by significantly decreased alpha diversity metrics for both bacteria and fungi communities. Notably, Shannon and Simpson indices calculated for bacteria communities reversed the downward trend at dpa30 unlike fungal communities. As the axolotl regrows its regenerated limb during this stage, it becomes apparent that the fungal community struggles to recover its original diversity post-treatment. Notably, however, Fungi and bacteria often have different life cycles and growth rates, and regeneration stages might favour bacterial growth or alters resource availability in a way that benefits bacteria over fungi, contributing to the disparity in alpha diversity metrics. Moreover, although the fungi community significantly shifts during the course of limb regeneration as manifested by the PERMANOVA main test the specific pairwise differences between

FIGURE 6 (A) Longitudinal shifts of bacterial taxa across axolotl limb regeneration. Longitudinal shifts of bacterial taxa across axolotl limb regeneration are depicted using LOESS regression fitting, which applies weighted local polynomials to model species abundance data over time. The visualisation showcases the longitudinal shifts of the Top20 taxa. Solid lines indicate the LOESS moving average, while shaded areas represent the 95% confidence interval around the fitted curve. (B) Analysis of indicator species in axolotl limb regeneration samples. Examination of indicator species within axolotl limb regeneration samples reveals distinct enrichment patterns at the ASV level. Only indicator values of high significance (IndVal >0.8, $p < 0.05$) are depicted. The colour scale bar indicates the indicator value for each ASV, while the size of the bubble symbol corresponds to the mean relative abundance of indicator ASVs.

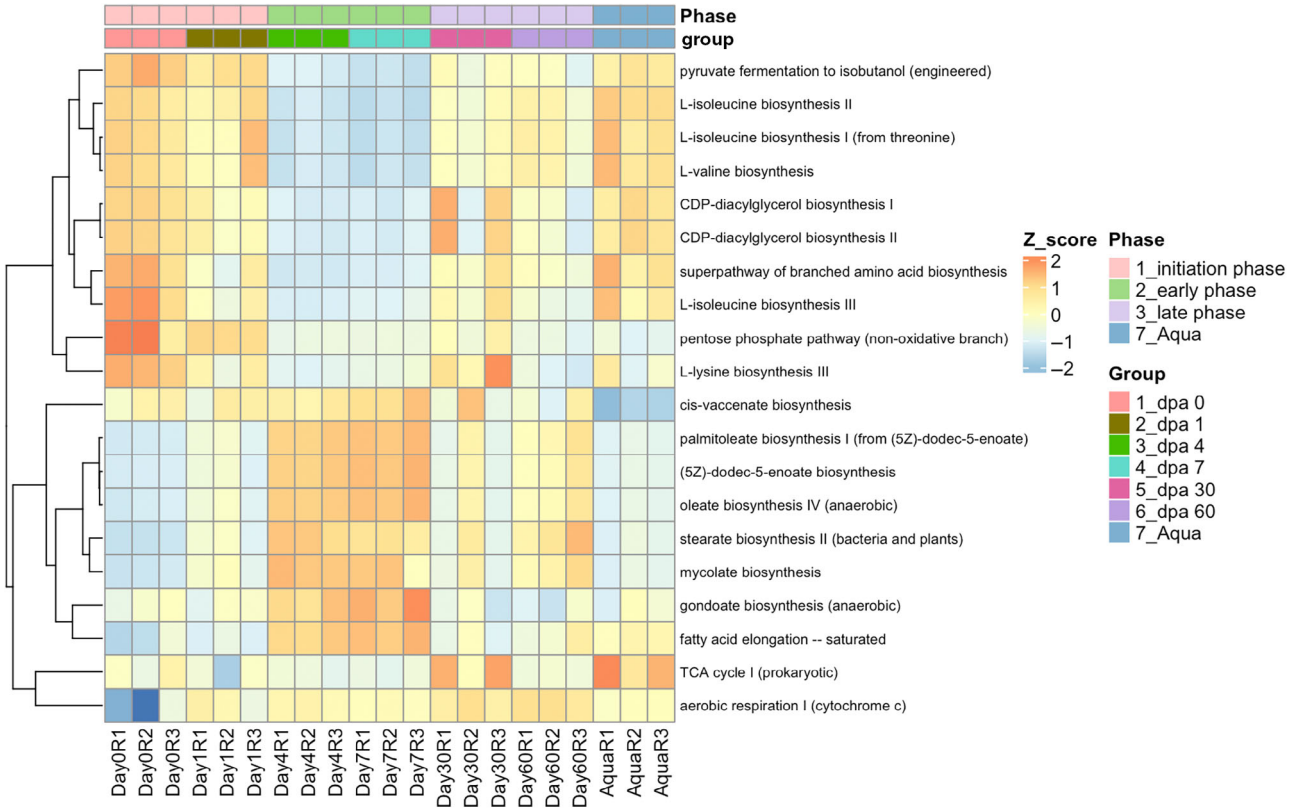

FIGURE 7 Heatmap of KEGG functional pathways predicted by PICRUSt2. The top 20 most prevalent functional pathways were clustered using complete-linkage hierarchical clustering employing Ward's method. The relative abundance values have been row-normalised and centered.

individual groups were not statistically significant. Even though this finding can be attributed to the small sample size (three replicates) for each pairwise comparison leading to limited power to detect true effects the hierarchical clustering of the samples was not congruent with the stage specific separation. Axolotl limb fungi may therefore have yet unknown subtle ecological complexity in responding to traumatic amputation and regeneration processes.

Flavobacterium, among other microbiota, warrants special attention during the course of limb regeneration as our results indicated this bacterium blooms across dpa4-dpa7 where the wound epithelium thickens and forms an apical epithelial cap, which promotes the generation of a population of undifferentiated mesenchymal cells called a 'blastema'. As a result, signals from the host and environmental cues can potentially promote or hinder differentiation and/or proliferation of the blastema cells in this critical stage. *Flavobacterium* belongs to the family *Flavobacteriaceae* in the phylum *Bacteroidota*. It is a Gram-negative genus comprising 270 species, ubiquities in the environment, including soil, seawater, freshwater, plants, and glaciers.[28,29] Many species of the genus *Flavobacterium* are capable of plant growth-promoting ability, hydrolyzing organic polymers, such as complex polysaccharides, cold-adapted species produce polyunsaturated fatty acids,[28] although some species (such as *F. columnare* and *F. psychrophilum*) reportedly cause infectious diseases in freshwater fish.[30,31] Nonetheless, considering axolotl was able to complete limb regeneration in this experiment in spite of the bloom of this bacterium the unknown species of *Flavobacterium* in this context may be positively contributing to the regeneration. Our core microbiota analysis (data not shown) showed that *Bacteriodes* and *Akkermansia*; *Flavobacterium*, and *Pseudomonas* and unclassified *Burkholderiaceae* were the top core members in the regeneration phases, respectively (initiation, early, and late phases) of axolotl used in our study. Remarkably, these taxa were found to be top most abundant bacteria colonising axolotl host in the natural environment,[32] further supporting the hypothesis that Flavobacterium is likely to play critical role in its regenerative capacity and/or protection of predator species. Even though skin microbiota of axolotl in their natural environment significantly changes by seasonal variation of abiotic factors such as temperature, pH, dissolved oxygen and conductivity and metamorphic status of the host[33] core microbiota and their genes[34] may be preserved if there is mutual biological benefit for both host and microbe regardless to seasonal changes.[35]

While its putative contribution to regenerative mechanisms and epigenetic and antigenic interactions with blastema cells cannot be ruled out evidence in the published literature support that beneficial cutaneous bacteria on amphibians protect against the lethal disease chytridiomycosis caused by *B. dendrobatidis* and salamanders.[36–40] In this study, our analysis of the fungal community did not detect Bd with the caveat that the majority of the ITS reads were not assigned to Unclassified Fungi. We therefore reasoned that either ITS primers did not amplify Bd, if present, or *Flavobacterium* might compete

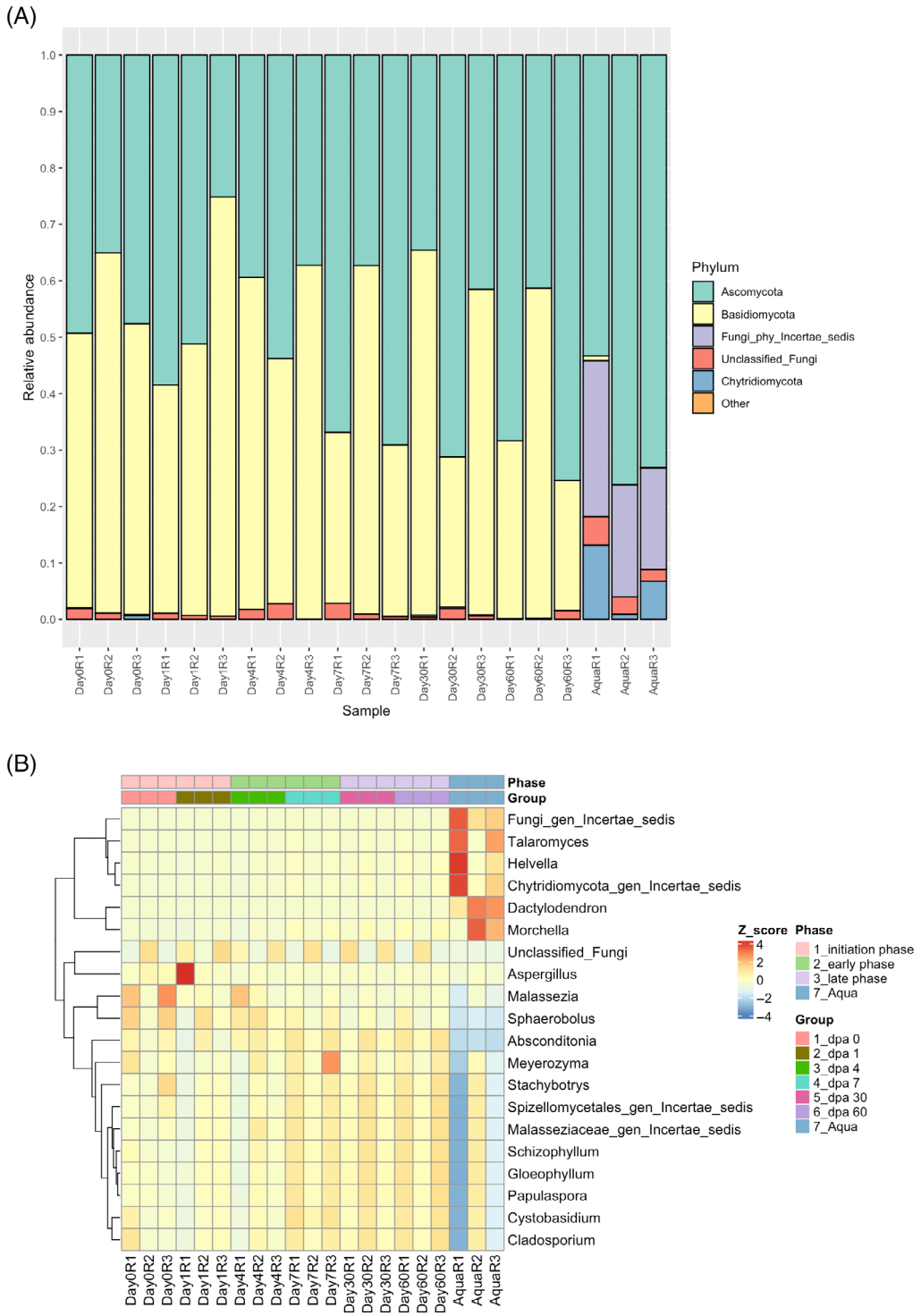

FIGURE 8 Fungal taxa dynamics during axolotl limb regeneration. (A) Stacked bar plot illustrating the relative abundance of the top five fungal phyla in samples from axolotl limb regeneration. (B) Heatmap displaying the top 20 fungal taxa using complete-linkage hierarchical clustering (Ward's method).

against unknown fungal species that could potentially impede regeneration mechanisms. Moreover, the prevalence of *Flavobacterium* exhibited a robust correlation with pathways related to lipid metabolism (Figure S1), indicating a potential role for this bacterium in influencing regeneration through lipid metabolic processes. Interestingly, a recent study analysed the metabolomic profile of axolotl blastema at dpa11.[41] Lipid metabolites such as sphingomyelin and sphingosine, along with polyamine and pyrimidine metabolism, were found to be enriched in blastema tissue. A recent cutaneous microbiota study on Ozark hellbender salamander subspecies

(*Cryptobranchus alleganiensis bishopi*), suffering from chronic wounds within their aquatic habitat has uncovered interesting findings.[42] The study showed that *Acidovorax* sp., *Flavobacterium* sp., *Aquabacterium* sp., *Chryseobacterium* sp., and *Acinetobacter* sp. were found to have higher relative abundance within these wounds compared to intact skin. These results are consistent with our own research, as all four species were identified as indicator species during axolotl limb regeneration studies. Nonetheless, further investigation is needed to determine whether these bacterial species, particularly *Flavobacterium*, are associated with the regenerative capacity of the axolotl limb.

The stage-specific restructuring of bacteria and fungi communities across the limb regenerating phases is fascinatingly chaotic and unstable as we found largely unique ASVs at almost every dpa timepoint (Figure 8A,B). Given that the wound epidermis covers the wound within a few hours of amputation and Apical Epithelial Cap (AEC) cells quickly develop in the initiation phase the newly colonising microbial communities at each dpa point would first have a chance to briefly interact with the wound epidermis but subsequently AEC cells during the critical stage of blastema proliferation. Even though the chaotic stage-specific restructuring of microbial communities can be due partly to microbial resource competition the host factors are likely in control of the community composition, providing the microbes less than favourable environment to form continuous biofilms at least until the re-developmental stage is completed. The host factors include the proinflammatory immune response to amputation and regeneration. Indeed, macrophages infiltrate the amputation site about the same time the wound epidermis covers the amputation site and depletion of macrophages impedes limb regeneration.[43] Theoretically, genetic and epigenetic signalling between macrophages, AEC cells, nerve cells, blastema, oxidative stress, and ultimately redecoration of limb skin with a protective mucus layer all would have an impact on the restructuring of the microbial community attempting to re-colonise regenerating tissues.

5 | CONCLUSIONS

Our findings offer compelling evidence for the first time that both bacterial and fungal communities undergo restructuring across the widely accepted three major phases in axolotl limb regeneration. However, it is noteworthy that the restructuring of the fungal community is less precisely congruent with the timing of these major phases. The notable bloom of *Flavobacterium* during the critical stage of blastema proliferation, along with the compositional shift of fungi from Basidiomycota dominance in the early phase to Ascomycota dominance in the late phase, raises intriguing questions about their potential impact on regenerative mechanisms in the limb tissues through unknown mechanisms. Future research, therefore, should investigate the contribution of microbial communities to regenerating tissues, specifically the cross talk between *Flavobacterium* and macrophages, and AEC cells. By unravelling these intricate interactions, we can gain deeper insights into the role of microbiota in the complex process of tissue regeneration, paving the way for potential therapeutic interventions that harness the therapeutic potential of microbial communities in enhancing tissue repair and regeneration.

AUTHOR CONTRIBUTIONS

Conceptualization: SY and TD. Data curation: HA and SY. Formal analysis: SY, BD, and HA. Methodology and resources: TD, BY, and SY. Writing – original draft: SY, Writing – review & editing: SY, TD, HA, and BY. All authors read and approved the final manuscript.

ACKNOWLEDGEMENTS

The financial support for this study was provided by the Medipol University Research Fund. We extend our gratitude to Ms. Ayça Önal and Ms. Damla Yay for their invaluable assistance in capturing axolotl limb photographs.

CONFLICT OF INTEREST STATEMENT

The authors have no conflicts of interest to declare.

DATA AVAILABILITY STATEMENT

The data that support the findings of this study are openly available in the NCBI Bio project at https://www.ncbi.nlm.nih.gov/bioproject/PRJNA1073213.

ORCID

Hanne Altın https://orcid.org/0000-0001-6068-3892
Büşra Delice https://orcid.org/0009-0007-2444-6380
Berna Yıldırım https://orcid.org/0000-0002-4479-2586
Süleyman Yıldırım https://orcid.org/0000-0002-2752-1223

REFERENCES

1. Tajer B, Savage AM, Whited JL. The salamander blastema within the broader context of metazoan regeneration. *Front Cell Dev Biol*. 2023; 11:1206157.
2. Echeverri K, Fei J, Tanaka EM. The Axolotl's journey to the modern molecular era. *Curr Top Dev Biol*. 2022;147:631-658.
3. Boluk A, Yavuz M, Demircan T. Axolotl: a resourceful vertebrate model for regeneration and beyond. *Dev Dyn*. 2022;251:1914-1933.
4. Endo T, Bryant SV, Gardiner DM. A stepwise model system for limb regeneration. *Dev Biol*. 2004;270:135-145.
5. McCusker C, Bryant SV, Gardiner DM. The axolotl limb blastema: cellular and molecular mechanisms driving blastema formation and limb regeneration in tetrapods. *Regeneration (Oxf)*. 2015;2:54-71.
6. Tank PW, Carlson BM, Connelly TG. A staging system for forelimb regeneration in the axolotl, *Ambystoma mexicanum*. *J Morphol*. 1976; 150:117-128.
7. Min S, Whited JL. Limb blastema formation: how much do we know at a genetic and epigenetic level? *J Biol Chem*. 2023;299:102858.
8. Wang MH, Hsu CL, Wu CH, et al. Timing does matter: nerve-mediated HDAC1 paces the temporal expression of morphogenic genes during axolotl limb regeneration. *Front Cell Dev Biol*. 2021;9: 641987.
9. Haas BJ, Whited JL. Advances in decoding axolotl limb regeneration. *Trends Genet*. 2017;33:553-565.
10. Gardiner DM, Muneoka K, Bryant SV. The migration of dermal cells during blastema formation in axolotls. *Dev Biol*. 1986;118:488-493.
11. Yokoyama H. Initiation of limb regeneration: the critical steps for regenerative capacity. *Dev Growth Differ*. 2008;50:13-22.

12. Diaz Heijtz R, Wang S, Anuar F, et al. Normal gut microbiota modulates brain development and behavior. *Proc Natl Acad Sci U S A*. 2011; 108:3047-3052.
13. Motta EVS, Moran NA. The honeybee microbiota and its impact on health and disease. *Nat Rev Microbiol*. 2023;22:122-137.
14. Panwar RB, Sequeira RP, Clarke TB. Microbiota-mediated protection against antibiotic-resistant pathogens. *Genes Immun*. 2021;22: 255-267.
15. Mure A, Sugiura Y, Maeda R, et al. Identification of key yeast species and microbe-microbe interactions impacting larval growth of Drosophila in the wild. *Elife*. 2023;12:RP90148.
16. Diaz-Diaz LM, Rodriguez-Villafane A, Garcia-Arraras JE. The role of the microbiota in regeneration-associated processes. *Front Cell Dev Biol*. 2021;9:768783.
17. Demircan T, Ilhan AE, Ovezmyradov G, Ozturk G, Yildirim S. Longitudinal 16S rRNA data derived from limb regenerative tissue samples of axolotl *Ambystoma mexicanum*. *Sci Data*. 2019;6:70.
18. Khattak S, Murawala P, Andreas H, et al. Optimized axolotl (*Ambystoma mexicanum*) husbandry, breeding, metamorphosis, transgenesis and tamoxifen-mediated recombination. *Nat Protoc*. 2014;9:529-540.
19. Usyk M, Zolnik CP, Patel H, Levi MH, Burk RD. Novel ITS1 fungal primers for characterization of the Mycobiome. *mSphere*. 2017;2: e00488.
20. Kechin A, Boyarskikh U, Kel A, Filipenko M. cutPrimers: a new tool for accurate cutting of primers from reads of targeted next generation sequencing. *J Comput Biol*. 2017;24:1138-1143.
21. Quast C, Pruesse E, Yilmaz P, et al. The SILVA ribosomal RNA gene database project: improved data processing and web-based tools. *Nucleic Acids Res*. 2013;41:D590-D596.
22. Nilsson RH, Larsson KH, Taylor AFS, et al. The UNITE database for molecular identification of fungi: handling dark taxa and parallel taxonomic classifications. *Nucleic Acids Res*. 2019;47:D259-D264.
23. Douglas GM, Maffei VJ, Zaneveld JR, et al. PICRUSt2 for prediction of metagenome functions. *Nat Biotechnol*. 2020;38:685-688.
24. McMurdie PJ, Holmes S. Phyloseq: an R package for reproducible interactive analysis and graphics of microbiome census data. *PLoS One*. 2013;8:e61217.
25. Weiss S, Van Treuren W, Lozupone C, et al. Correlation detection strategies in microbial data sets vary widely in sensitivity and precision. *ISME J*. 2016;10:1669-1681.
26. Friedman J, Alm EJ. Inferring correlation networks from genomic survey data. *PLoS Comput Biol*. 2012;8:e1002687.
27. Nowoshilow S, Schloissnig S, Fei JF, et al. The axolotl genome and the evolution of key tissue formation regulators. *Nature*. 2018;554:50-55.
28. Waśkiewicz A, Flavobacterium LI. spp. – characteristics, occurrence, and toxicity. In: Batt C, ed. *Encyclopedia of Food Microbiology*. 2nd ed. Academic Press; 2014.
29. Yang LL, Liu HC, Xin YH, Liu Q. Flavobacterium frigoritolerans sp. nov. and Flavobacterium shii sp. nov., isolated from glaciers on the Tibetan Plateau. *Int J Syst Evol Microbiol*. 2023;73:73.
30. Loch TP, Faisal M. Emerging flavobacterial infections in fish: a review. *J Adv Res*. 2015;6:283-300.
31. De Silva L, Heo GJ. Biofilm formation of pathogenic bacteria isolated from aquatic animals. *Arch Microbiol*. 2022;205:36.
32. Ramirez-Barahona S, Gonzalez-Serrano FM, Martinez-Ugalde E, Soto-Pozos A, Parra-Olea G, Rebollar EA. Host phylogeny and environment shape the diversity of salamander skin bacterial communities. *Anim Microbiome*. 2023;5:52.
33. Martinez-Ugalde E, Avila-Akerberg V, Gonzalez Martinez TM, et al. The skin microbiota of the axolotl Ambystoma altamirani is highly influenced by metamorphosis and seasonality but not by pathogen infection. *Anim Microbiome*. 2022;4:63.
34. Martinez-Ugalde E, Avila-Akerberg V, Gonzalez Martinez TM, Rebollar EA. Gene functions of the Ambystoma altamirani skin microbiome vary across space and time but potential antifungal genes are widespread and prevalent. *Microb Genom*. 2024;10:1-14.
35. Walke JB, Becker MH, Krinos A, et al. Seasonal changes and the unexpected impact of environmental disturbance on skin bacteria of individual amphibians in a natural habitat. *FEMS Microbiol Ecol*. 2021; 97:fiaa248.
36. Bataille A, Lee-Cruz L, Tripathi B, Kim H, Waldman B. Microbiome variation across amphibian skin regions: implications for Chytridiomycosis mitigation efforts. *Microb Ecol*. 2016;71:221-232.
37. Bates KA, Clare FC, O'Hanlon S, et al. Amphibian chytridiomycosis outbreak dynamics are linked with host skin bacterial community structure. *Nat Commun*. 2018;9:693.
38. Bates KA, Sommer U, Hopkins KP, et al. Microbiome function predicts amphibian chytridiomycosis disease dynamics. *Microbiome*. 2022;10:44.
39. Muletz Wolz CR, Yarwood SA, Campbell Grant EH, Fleischer RC, Lips KR. Effects of host species and environment on the skin microbiome of Plethodontid salamanders. *J Anim Ecol*. 2018;87:341-353.
40. Shaw SD, Berger L, Bell S, et al. Baseline cutaneous bacteria of free-living New Zealand native frogs (Leiopelma archeyi and Leiopelma hochstetteri) and implications for their role in defense against the amphibian chytrid (*Batrachochytrium dendrobatidis*). *J Wildl Dis*. 2014; 50:723-732.
41. Liu Z, Li W, Geng L, et al. Cross-species metabolomic analysis identifies uridine as a potent regeneration promoting factor. *Cell Discov*. 2022;8:6.
42. Hill AJ, Grisnik M, Walker DM. Bacterial skin assemblages of sympatric salamanders are primarily shaped by host genus. *Microb Ecol*. 2023;86:1364-1373.
43. Godwin JW, Pinto AR, Rosenthal NA. Macrophages are required for adult salamander limb regeneration. *Proc Natl Acad Sci U S A*. 2013; 110:9415-9420.

SUPPORTING INFORMATION

Additional supporting information can be found online in the Supporting Information section at the end of this article.

How to cite this article: Altın H, Delice B, Yıldırım B, Demircan T, Yıldırım S. Temporal microbiome changes in axolotl limb regeneration: Stage-specific restructuring of bacterial and fungal communities with a *Flavobacterium* bloom during blastema proliferation. *Wound Rep Reg*. 2024;32(6): 826-839. doi:10.1111/wrr.13207